High Pressure Die Cast nAlN reinforced AZ91 Magnesium Alloy

Mahfuz Karim*, Guangyu Liu, Dmitry Eskin, Brian McKay

Brunel Centre for Advanced Solidification Technology, Brunel University London, Uxbridge, Middlesex, UB8 3PH

*Corresponding email address: mahfuz.karim@brunel.ac.uk

Abstract
Magnesium alloys strengthened with ceramic particles have been extensively researched as a lightweight, high strength alternative to other structural alloys, such as steel and aluminium. They are important in industries where a low density and a high strength are essential, such as the aerospace and automotive industries. In this study, an AZ91+0.75 wt% AlN electrical nanocomposite housing was produced by combining a magnesium AZ91 alloy with an Al-20 wt% nAlN masteralloy through stir-casting, ultrasonication, and high-pressure die casting. The housing component was selected as a model to demonstrate industrial applicability. Microstructures of the as-cast, nanocomposite components have been examined, and their resultant mechanical properties analysed and discussed.

Keywords: Magnesium MMnCs, nAlN particles, stir casting, ultrasonication, HPDC, microstructure, mechanical properties

1 Introduction
The use of magnesium metal matrix composites (MMMCs) has experienced significant growth in the automotive and aerospace industries. This growth can be attributed to their remarkable properties that include low density and high strength [1]. Magnesium's low density, which is two-thirds that of Al and one-fifth that of steel, makes it a desirable material for achieving weight reduction. The AZ series of magnesium alloys are widely used commercially for applications such as automotive front engine cover, electrical housing, and aerospace engine frames as they also exhibit excellent castability, damping capacity, and high machinability [2]. Desirable properties can be further enhanced by the careful selection of reinforcement materials. This reinforcement can be categorized as fibres, whiskers, or particles. Particle reinforced MMMCs are increasingly preferred because they are cost-effective and easier to produce than other reinforcement types and provide isotropic mechanical characteristics. The most commonly used reinforcements are silicon carbide (SiC) [3][4], aluminium oxide (Al_2O_3) [5], titanium carbide (TiC) [6], boron carbide (B4C) [7], and aluminium nitride (AlN) [8]. Specifically, AlN ceramic particles possess desirable structural characteristics and thermophysical properties, including high melting point, high hardness, high strength, good thermal conductivity, and low thermal expansion coefficient, making it a highly suitable reinforcement for Mg alloys [9][10][11].

The performance of composite material is dependent on the distribution of the particles within the matrix and the strength of the matrix/reinforcement bonding. Nanoparticles in powder form exist as an agglomeration which creates defects and failure stress points within the matrix. The use of a masteralloy containing the reinforcement particles promotes the introduction and dispersion of the particles in the liquid matrix. The dispersion of the nanoparticles in the molten melt requires a shear force to break agglomerations. These forces can arise from the stir casting, ultrasonic cavitation effect and the high pressure die casting process, thus enabling discrete particles to be distributed within the matrix. During ultrasonication, acoustic waves generate stress within the molten melt forming cavities called cavitation bubbles. Temperatures of several thousand degrees and pressures of up to a thousand atmospheres can be

created during the short life of the collapsing cavitation bubble. When the bubbles implode the force created from shock waves on the particles may be greater than the van der Waal's force agglomerating the particles, resulting in the brake-up of the agglomerations [12].

In this study, nAlN reinforced magnesium composites are produced by a combination of stir casting, ultrasonication and high pressure die casting, to produce an electrical housing component. An Al-20 wt% nAlN masteralloy made by high energy ball milling is incorporated to improve the dispersion of nAlN particle within the matrix. The subsequent composite mechanical properties in the component are investigated, and the findings are discussed.

2 Materials & Methods

2.1 Materials

AZ91 magnesium alloy and AlN reinforcement particles were used in the fabrication of the composite material, with the nominal composition of the "as-received" commercial alloy given in Table 1. The masteralloy was produced by high-energy ball milling (HEBM) and supplied by MBN Nanomaterialia (Italy). The particle size distribution range in the Al-20 wt% nAlN masteralloy was 50-100 nm. The elemental composition of the composite material was kept the same as the base alloy with the exception of the 0.75 wt% nAlN addition.

Table 1: AZ91 Composition (wt%)

AZ91	Mg	Al	Zn	Mn	Si	Cu	Fe	Ni
wt%	Remainder	9.0	0.7	0.3	0.1	0.03	0.005	0.002

2.2 Component Production

Figure 1 shows the schematic experimental flow for producing the nAlN reinforced AZ91. A Carbolite Gero 301 top loading heat resistance chamber furnace was used to produce Mg melt at 690±5°C and a N2+cover gas (R134a) was employed to protect the Mg from oxidising. The casting temperature of AZ91 for HPDC is typically 670±5°C, however for the composite a higher temperature 680±5°C was required due to the increase in viscosity of the melt. The masteralloy Al-20% nAlN was preheated to 300°C for 1-2 hrs prior to casting, to remove moisture. Mechanical stirring was conducted simultaneously with the masteralloy addition to the melt. The impeller (50 mm diameter) was positioned one third from the bottom of the crucible and rotated at a speed of 400-500 rpm (which was adjusted to maintain a vortex). After the masteralloy was completely added, the melt was placed back into the furnace for reheating to compensate for the heat loss arising from mixing. Once the temperature was above 690°C, ultrasonication processing of the melt was performed at 17 kHz and 3.5 kW power for 20 mins using a niobium sonotrode. When the melt was stabilised at the casting temperature, the Mg composite melt was transferred by a steel ladle and poured into the shot sleeve to start HPDC casting. A Frech DAK 1600-133 cold chamber machine with a locking force of 4800 kN and plunger velocity at 3.6 m/s was used. An AZ91 base alloy and an AZ91 + 0.75 wt% nAlN composite component were produced. The casting process can be thus divided into three stages: pre-mixing of AlN masteralloy by mechanical stirring, further dispersion by ultrasonication, and HPDC casting as shown in Figure 2.

Figure 1: Schematic experimental flow: Melt Preparation>NPs Introduction (Mixing)>Reheating>Ultrasonic Treatment>Melt Stabilisation>Casting

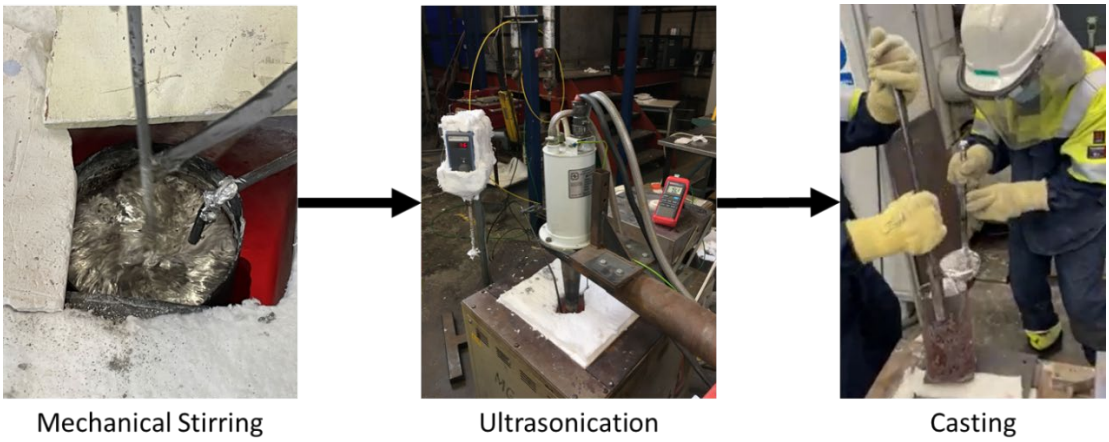

Figure 2: Composite Casting Procedure: Mechanical Stirring, Ultrasonication and Casting

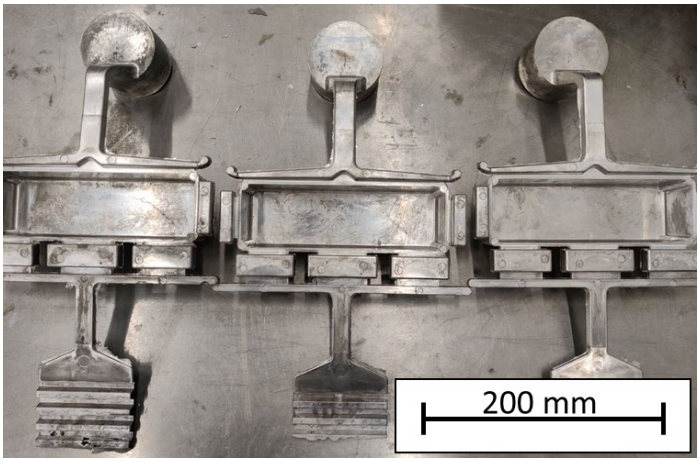

Figure 3: Electrical Housing Component Castings

3 Results & Discussion

Figure 4a, 4b, and 4c presents TEM micrographs showing the size and morphology of AlN nanoparticles and 4d presents an SEM secondary electron micrograph showing the size, morphology, and distribution of nAlN particles in the Al-20 wt% nAlN masteralloy microstructure. The nAlN particles show a faceted polyhedral morphology and particle diameter range of 50-100 nm, with a mean average of 70 nm.

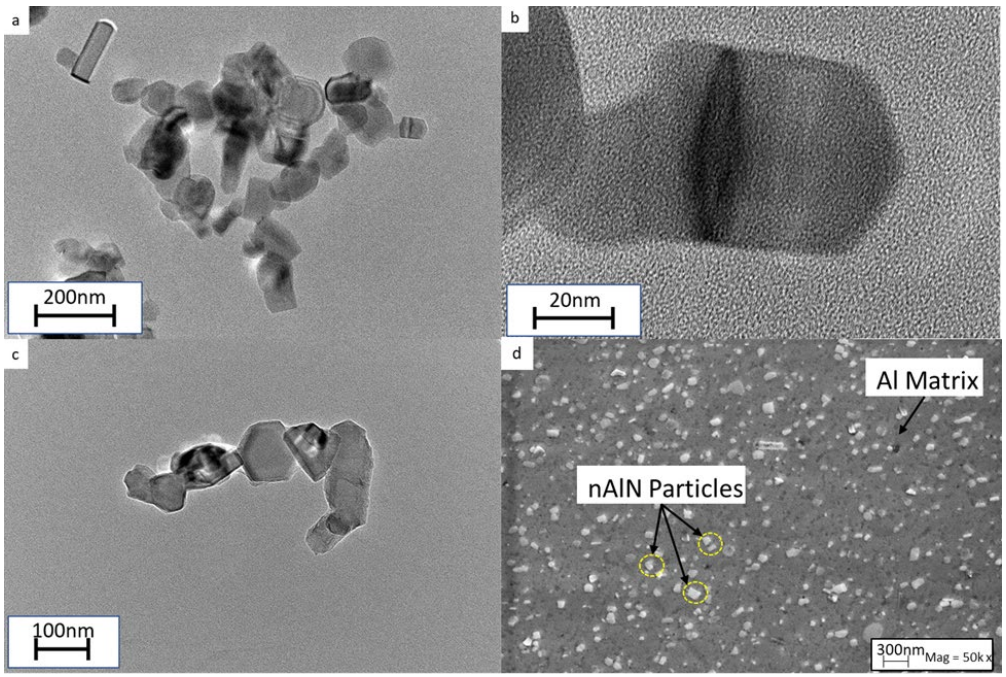

Figure 4: (a), (b) and (c) TEM micrographs of loose nAlN particles exhibiting a faceted polyhedral morphology and particle size of 50-100 nm; (d) SEM micrographs of the Al-20 wt% nAlN masteralloy with a good distribution of particles and no evidence of major defects such as cracks or sintered particles.

Figure 5a and 5b gives the SEM secondary electron micrographs at high magnification, showing that the primary and secondary phases are both present within the alloy, in addition to the particles in the composite. Figure 5c and 5d present the SEM back-scattered micrographs showing the main phases of AZ91 alloy and nAlN present in the microstructure. The SEM-BSD micrographs revealed that microstructure consists of α-Mg, β-Mg and AlMn phases. The nAlN particles are distributed throughout the microstructure and although clusters are regularly present within it as shown in Figure 5b. there seems to be no reagglomeration of the particles by van der Waal forces, during the solidification process. A confirmation of AlN was made by EDS spot analysis on the individual nanoparticles as shown in Figure 6, where the indication of a nitrogen peak confirms an AlN presence. The detailed in-depth examination of nAlN particle size and chemistry will be conducted in future studies.

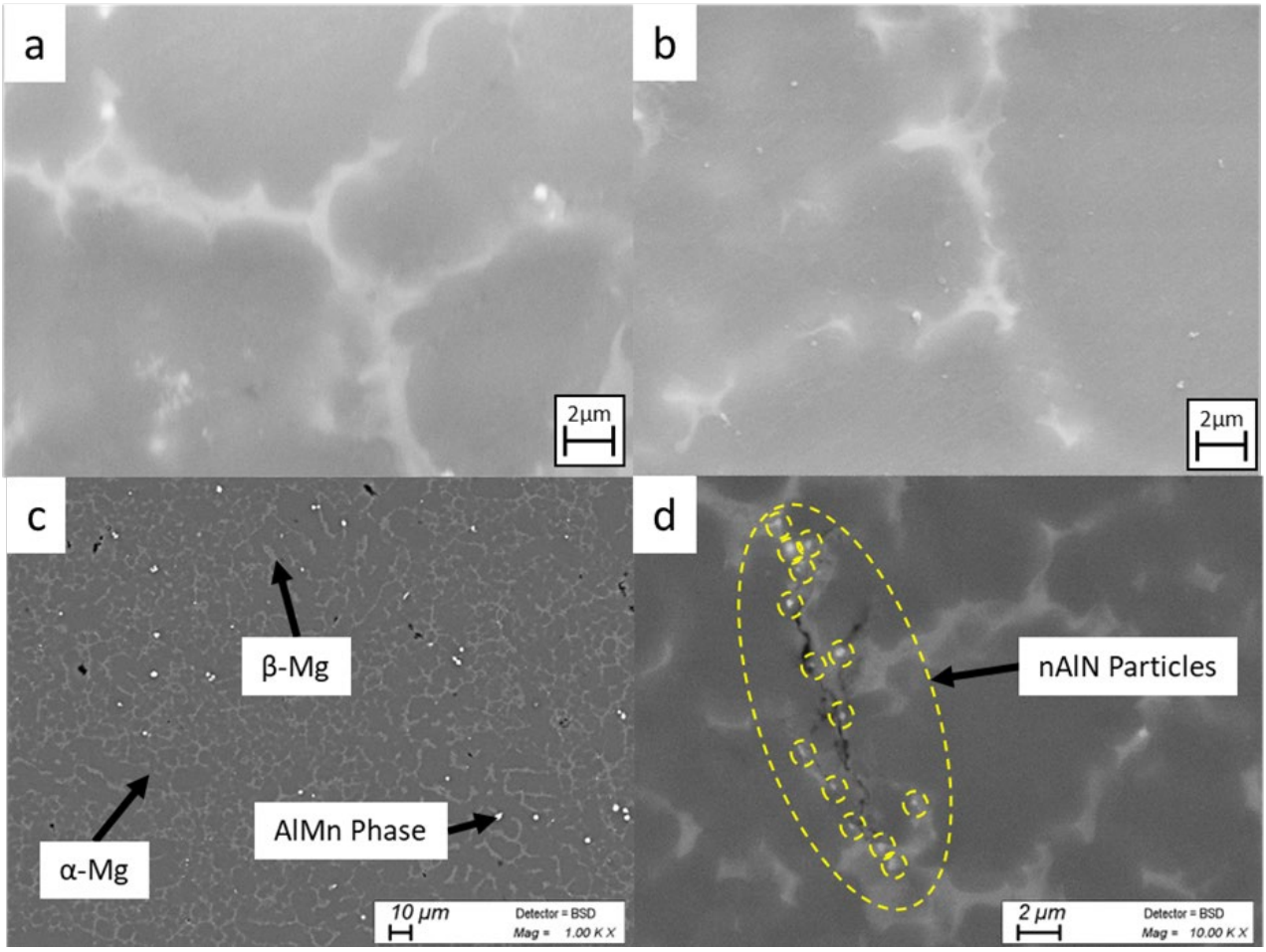

Figure 5: (a) SEM-SE micrograph of AZ91; (b) SEM-SE micrograph of AZ91+0.75 wt% nAlN (c) SEM-BSD of AZ91 + 0.75 wt% NP; Three phases observed α-Mg, β-Mg and AlMn intermetallic; (d) Clusters of nAlN particles observed but no agglomerations exist

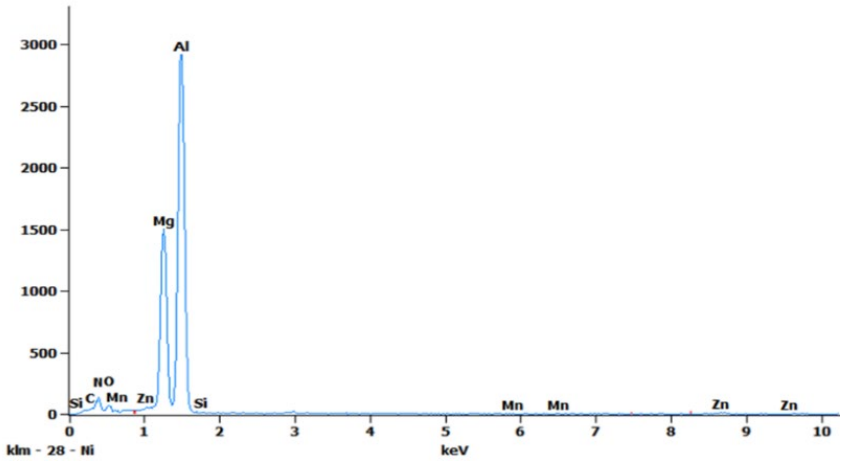

Figure 6: Elemental spectrum of AZ91_0.75wtr%nAlN, with nitrogen peak indicating the presence of AlN

The addition of AlN into AZ91 has shown that the nanoparticles have been dispersed throughout the component, which is partially attributed to the use of the Al-20 wt% nAlN masteralloy. The finding also suggests that the dispersion of the nanoparticles was obtained by the combination of stir casting, ultrasonication and HPDC processes. However, some particle clusters observed within the microstructure indicate that the dispersion of the particles was not fully uniform throughout the component. The solidification interaction of the nAlN within the melt determines the engulfment by the solidification front or the pushing of the front towards the grain boundaries [13]. The engulfment of particles is the beneficial phenomenon which leads to particles strengthening the material, whilst the pushing of particles into the grain boundaries leads to a minimal strengthening effect and the creation of defect locations. The main conditions required to engulf particles are the repulsive force from the interfacial energy and the drag force from the liquid flow. Therefore, it has been suggested that a critical solidification front velocity is required to engulf a critical particle size when the two opposing forces are equal [14][15]. In this sense the AlN nanoparticles present within the grain indicate that the critical particle size has been met for the solidification front to engulf the particles and disperse them into the matrix. On the other hand, no reagglomeration was observed thereby suggesting that the pushing of particles was not significant, indicating the fluid force is greater or equal to the weak attraction force between particles. In addition, the wettability of the matrix and nanoparticles could have been improved by the use of the masteralloy where the particles were pre-mixed within an aluminium matrix. The detailed in-depth microscopic examination of nAlN/AZ91 matrix interfacial features and behaviour associated with mechanical strengthening will be conducted in future studies.

3.1 Mechanical Properties

Figures 7 and 8 show the tensile properties including the YS, UTS and elongation of the base alloy AZ91 and nAlN reinforced AZ91 composite alloy. The YS of AZ91 was 146±6 MPa, which increased to 184±21 MPa for the AZ91+0.75 wt% nAlN composite. The composite with the nanoparticle addition has thus shown an average increase of 25% compared with the base material. Also, the UTS of AZ91 was 167±18 MPa, which increased to 190±10 MPa yielding an average increase of 14%. An overlap in the range of YS and UTS values was observed between the composite and the base alloy. The elongation of the AZ91 was 1.2%±0.6%, which decreased to 0.8±0.3% with the addition of AlN particles. The range of data produced was consistent, indicating a good distribution of particles. The composite material has shown an increase in strength but reduction in ductility. This can be associated with the strengthening mechanism, in particular CTE, where the difference in coefficients of thermal expansion of the Mg alloy and AlN nanoparticle led to a greater number of dislocations being generated. This causes a high work hardening effect and thus a strengthening effect, but also leads to the ductility decrease. Due to these locations acting as stress concentrators, the propagation of fracture is more likely occur. The material goes through a shorter plastic deformation; thus, the elongation is reduced. The distribution of the particles throughout the matrix allows for the particle strengthening mechanism to occur throughout the material thus increasing the YS by 25%. The optimum wt% of AlN nanoparticle reinforcement to AZ91 will be further investigated in future. Figure 9 shows the Vickers hardness of the AZ91 and AZ91+0.75 wt% nAlN HPDC components. The hardness value for AZ91 base alloy was measured to be 65±2 HV, which increased to 96±5 HV when reinforced by 0.75wt% of nAlN, an increase of 47%.

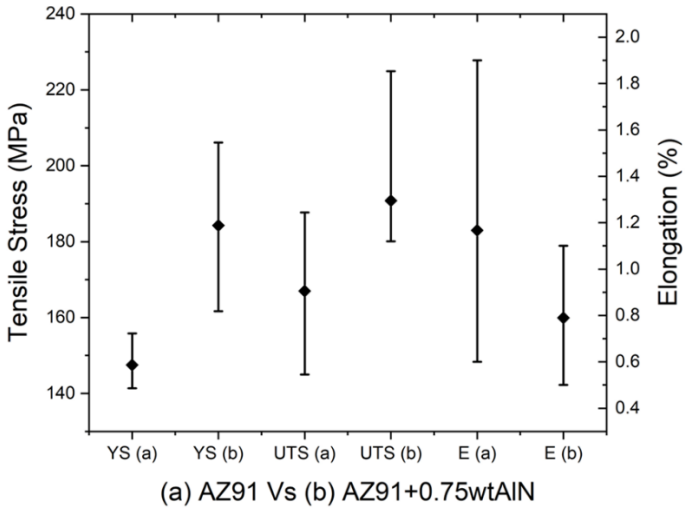

Figure 7: Tensile properties of (a) AZ91 and (b) AZ91+0.75wt%nAlN; yield strength (YS), ultimate tensile stress (UTS) and elongation (E) with error bars plotted.

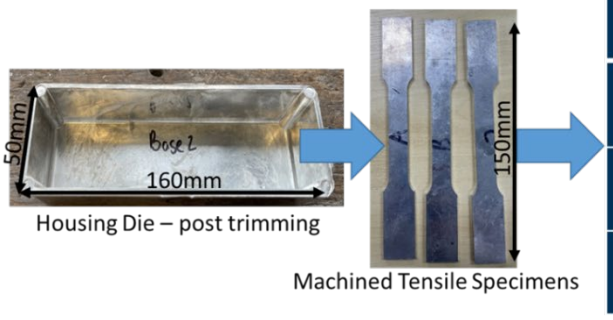

Property \ Material	AZ91	AZ91 + 0.75wt% nAlN
Yield Strength (0.2% Proof Stress)	147.5 ± 6 MPa	184 ± 21 MPa (+25%)
UTS	167 ± 18 MPa	190 -10+34 MPa (+14%)
Elongation	1.9% (max)	1.1% (max)

Figure 9: Transition from component to tensile specimens

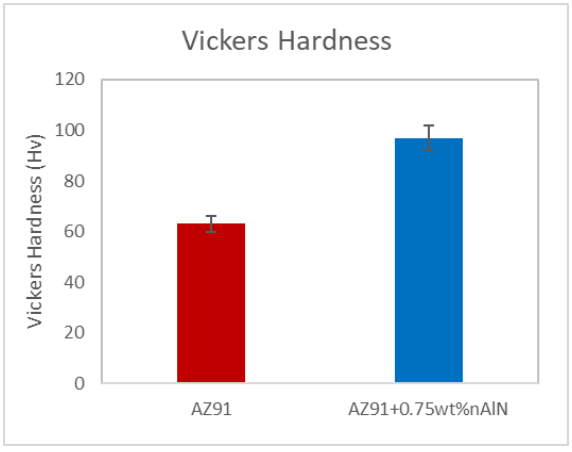

Figure 9: Vickers Hardness of AZ91 alloy and AZ91 reinforced with 0.75wt%nAlN

4 Conclusions

The current work produced an AZ91 composite electric housing component reinforced with 0.75 wt% nAlN that was added from a masteralloy, Al-20 wt% nAlN, through a combination of stir casting, ultrasonication and high pressure die casting. The study attempts to explore the effects of AlN nanoparticles on the microstructure and mechanical properties of high pressure die cast AZ91 components. The following conclusion can be drawn:

- Nanoparticles have been dispersed throughout the composite reinforced with AlN nanoparticles with minimal particle clusters present and no reagglomerations.
- The YS and UTS was improved by 25% and 14%, respectively, with the addition of 0.75 wt% AlN nanoparticles due to the coefficient of thermal expansion strengthening mechanism. The elongation was reduced from an average of 1.2% to 0.8% due to the work hardening effect from the strengthening mechanism which influences the plastic deformation of the material.
- The Vickers hardness was improved by 47% with the reinforcement of 0.75wt% nAlN.

References

1. Dey, A. and Pandey, K.M., 2015. Magnesium metal matrix composites-a review. Rev. Adv. Mater. Sci, 42(1), pp.58-67.
2. Abbas, A., Rajagopal, V. and Huang, S.J., 2021. Magnesium metal matrix composites and their applications. Magnesium alloys structure and properties.
3. Bagheri, B., Abbasi, M., 2020. Development of AZ91/SiC surface composite by FSP: effect of vibration and process parameters on microstructure and mechanical characteristics. Adv. Manuf. 8, 82–96.
4. Behrouz B, Mahmoud A, Amin A, Seyyed E.M., 2020. Effect of second-phase particle size and presence of vibration on AZ91/SiC surface composite layer produced by FSP, Transactions of Nonferrous Metals Society of China, pp.905-916.
5. Ahmadkhaniha, D., Sohi, M.H., Salehi, A. and Tahavvori, R., 2016. Formations of AZ91/Al2O3 nano-composite layer by friction stir processing. Journal of Magnesium and Alloys, 4(4), pp.314-318.
6. Kumar, A., Kumar, S., Mukhopadhyay, N.K., Yadav, A., and Sinha, D.K., 2022. Effect of TiC reinforcement on mechanical and wear properties of AZ91 matrix composites. International Journal of Metalcasting, 16(4), pp.2128-2143.
7. Singh, N., Singh, J., Singh, B. and Singh, N., 2018. Wear behavior of B4C reinforced AZ91 matrix composite fabricated by FSP. Materials Today: Proceedings, 5(9), pp.19976-19984.
8. Kumar, S.S. and Mohanavel, V., 2022. An overview assessment on magnesium metal matrix composites. Materials Today: Proceedings, 59, pp.1357-1361.
9. Sun, Y., Yang, C., Zhang, B., Fan, J., Li, H., Zhao, T. and Li, J., 2022. The aging behavior, microstructure, and mechanical properties of AlN/AZ91 composite. Journal of Magnesium and Alloys.
10. Bedolla, E., Lemus-Ruiz, J. and Contreras, A., 2012. Synthesis and characterization of Mg-AZ91/AlN composites. Materials & Design, 38, pp.91-98.
11. Zhang, B., Yang, C., Sun, Y., Li, X. and Liu, F., 2019. The microstructure, mechanical properties, and tensile deformation mechanism of rolled AlN/AZ91 composite sheets. Materials Science and Engineering: A, 763, p.138118.
12. Dieringa, H., 2018. Processing of Magnesium-Based Metal Matrix Nanocomposites by Ultrasound-Assisted Particle Dispersion: A Review. Metals, [online] 8(6), p.431
13. Ferguson, J.B., Kaptay, G., Schultz, B.F. et al. 2014. Brownian Motion Effects on Particle Pushing and Engulfment During Solidification in Metal-Matrix Composites. Metall Mater Trans A 45, 4635–4645
14. Sen S, Dhindaw BK, Stefanescu DM, Catalina A, Curreri PA, 1997. Melt convection effects on the critical velocity of particle engulfment. J Cryst Growth 173(3-4):574-84.
15. Youssef YM, Dashwood RJ, Lee PD, 2005. Effect of clustering on particle pushing and solidification behaviour in TiB2 reinforced aluminium PMMCs. Compos. Part A Appl. Sci. Manuf. 36(6): 747-63.